Development 125, 3427-3436 (1998)
Printed in Great Britain © The Company of Biologists Limited 1998
DEV7637

Patterned epidermal cell death in wild-type and segment polarity mutant *Drosophila* embryos

Todd M. Pazdera[1], Prem Janardhan[2] and Jonathan S. Minden[1,*]

[1]Department of Biological Sciences and the Center for Light Microscope Imaging and Biotechnology and [2]Department of Computer Science, Carnegie Mellon University, Pittsburgh, PA 15213, USA
*Author of correspondence (e-mail: minden@cmu.edu)

Accepted 27 May; published on WWW 6 August 1998

SUMMARY

Programmed cell death plays an essential role in the normal embryonic development of *Drosophila melanogaster*. One region of the embryo where cell death occurs, but has not been studied in detail, is the abdominal epidermis. Because cell death is a fleeting process, we have used time-lapse, fluorescence microscopy to map epidermal apoptosis throughout embryonic development. Cell death occurs in a stereotypically striped pattern near both sides of the segment border and to a lesser extent in the middle of the segment. This map of wild-type cell death was used to determine how cell death patterns change in response to genetic perturbations that affect epidermal patterning. Previous studies have suggested that segment polarity mutant phenotypes are partially the result of increased cell death. Mutations in *wingless*, *armadillo*, and *gooseberry* led to dramatic increases in apoptosis in the anterior of the segment while a *naked* mutation resulted in a dramatic increase in the death of *engrailed* cells in the posterior of the segment. These results show that segment polarity gene expression is necessary for the survival of specific rows of epidermal cells and may provide insight into the establishment of the wild-type epidermal cell death pattern.

Key words: Apoptosis, Epidermis, Segment polarity genes, *Drosophila melanogaster*, *wingless*, *naked*

INTRODUCTION

Pattern formation during *Drosophila* embryogenesis requires specific numbers of cells to be established in each tissue primordia. The developing embryo must maintain a delicate balance between cell division and cell death to generate the appropriate number of cells. The patterns of cell division in the *Drosophila* embryo is very well understood (Hartenstein and Campos-Ortega, 1985; Foe, 1989). The proteins that regulate the *Drosophila* cell cycle are also well characterized (reviewed by Edgar and Lehner, 1996). However, little is known about the mechanism for regulating the global mitotic pattern, which gives rise to regions of synchronously dividing cells, known as mitotic domains. It is believed that these mitoses produce an excess of cells required for a viable embryo and that programmed cell death, or apoptosis, is necessary to remove these extraneous cells (reviewed by Jacobson et al., 1997). Cell death is essential for embryo survival and a number of genes that function in the apoptotic pathway are known. Embryos that are deficient for cell death fail at head involution (Grether et al., 1995) and show signs of hypertrophy in the central nervous system (White et al., 1994). Cell death also plays a role in repairing pattern defects. Mis-patterned embryos with increased numbers of abdominal cells, are repaired by the elimination of excess cells by apoptosis (Namba et al., 1997). There are two major gaps in our understanding of cell death in *Drosophila* embryos: (1) what is the wild-type pattern of cell death and (2) what are the signals that initiate the apoptotic programme?

One tissue where apoptosis is present, but has not been studied in detail, is the embryonic abdominal ectoderm, which gives rise to the highly patterned larval cuticle with its characteristic bands of ventral denticles and dorsal hairs. The arrangement of these structures is generated by the precise expression of patterning genes in the embryo. Segment polarity genes play a key role in establishing the fate of the cuticle secreting cells through cell signaling interactions between neighboring rows of cells in the ectoderm (reviewed by DiNardo et al., 1994; Martinez Arias, 1993). Establishing the appropriate numbers of cells in the epidermis is believed to be essential to produce a normal cuticle pattern. Too few or too many cells may result in abnormally sized structures, pattern disruption and potential lethality. Mutations in segment polarity genes lead to shortened embryos and increased epidermal cell death (Klingensmith et al., 1989; Perrimon and Mahowald, 1987). Given the intimate role of segment polarity genes in establishing embryonic epidermal fates, it is of interest to determine the role segment polarity genes play in initiating the apoptotic cell death that leads to the pruning of excess cells in the epidermis.

In order to gain a better understanding of the role of apoptosis in epidermal patterning, a map of the cell death in wild-type embryos was generated. Apoptosis first appears at embryonic stage 11 and persists throughout the remainder of embryonic development (Campos-Ortega and Hartenstein, 1985). Previous studies have shown that apoptosis is a relatively short-lived process where the dead cells are engulfed either by neighboring cells or migrating macrophages. Images of embryos that were fixed and stained for cell death hint at a segmentally repeated cell death pattern, but these snapshots are unable to capture the full pattern of this dynamic process. We have used time-lapse microscopy to record the spatial and temporal changes in cell death. These recordings provide a precise mapping of cell death over time, which clearly shows that epidermal cell death is repeated segmentally. In order to determine the location of these cell deaths within the segment, apoptosis was mapped with respect to segment borders and segment polarity gene expression in live embryos. We find that cell death in the epidermis occurs predominantly near the segment borders, near or in *engrailed (en)*-expressing cells and to a lesser extent in the middle of the segment.

The wild-type cell death map was used to compare the cell death profiles of a number of segment polarity mutant embryos. Mutations in the *wg* signaling pathway lead to the demise of several rows of cells in the anterior-most portion of the segment. Mutations in the segment polarity gene *naked* (*nkd*) also lead to a dramatic increase in apoptotic death in *en*-expressing abdominal cells. These results show that segment polarity mutants have an altered cell death pattern in a stereotypical manner, suggesting that these genes are important in determining epidermal cell survival.

MATERIALS AND METHODS

Stocks

Oregon R and *white* Canton S were used as wild-type stocks. A temperature sensitive allele of *wingless* ($wg^{1\text{-}12}$) (Nüsslein-Volhard and Wieschaus, 1984), was provided by Steve DiNardo. The $wg^{1\text{-}12}$ allele was maintained with a blue balancer chromosome carrying an *eve:lacZ* construct, which was used to determine homozygous mutant embryos. The *armadillo* temperature sensitive allele, $arm^{H8.6}$, was provided by Norbert Perrimon. Null mutants of *gooseberry* (Df(2R)*gsb*) (Li and Noll, 1993) and *naked* (nkd^2) (Perrimon, 1989) were provided by the Bloomington Stock Center.

Monitoring cell death, gene expression and segment borders in vivo

Stage 3 embryos were collected, mounted and injected as described previously (Namba et al., 1997). Cell death was visualized by injecting the embryos with a solution of 0.5 mg/ml acridine orange (AO) in PBS. To visualize *lac*Z expression, embryos were injected with a 1.5 mM solution of RGPEG (Minden, 1996). Segment borders were visualized by injecting embryos in the intervitelline space with RGPEG which fluoresces brightly when it accumulates in crevices on the embryo surface. Fluorescent, time-lapse recordings of injected embryos were generated starting at late stage 11. Each recording consisted of stacks of 4-6 images taken 5 μm apart, taken at 5-8 minute intervals for up to 12 hours. Embryo collection, maturation and recording temperatures are detailed in the Results section.

Identifying homozygous mutant embryos

Two methods were used to identify the genotype of mutant embryos: (1) mutants were identified by inspection of the cuticle pattern of stage 17 embryos. Cuticle preparations of injected embryos were performed in situ on the coverslip to maintain the relative position of the embryos to correlate cuticle phenotype with time-lapse images. Late stage embryos were injected in the intervitelline space with a 4:1 mixture of acetic acid: glycerin, incubated on a heating block at 65˚C for 30 minutes and then incubated overnight at room temperature. The halocarbon oil was scraped from the coverslip, covered with 1:1 CMC10 (Masters chemical):lactic acid, covered with a second coverslip and incubated overnight at 60˚C. (2) *wg* mutant embryos were identified by injecting stage 4 embryos with RGPEG into the syncytial cytoplasm to detect *eve:lacZ* expression from the balancer chromosome. Homozygous *wg* embryos lacked *eve:lacZ* expression.

Generation of cell death maps in wild-type embryos

The position of apoptotic cells when they first become AO positive was determined. For each time point of the time-lapse recording, 2-3 optical sections, taken 5 μm apart, were superimposed electronically. These images were contrast enhanced by applying a spot detection function, consisting of a scanning comparison box of the dimensions of a nucleus, which identifies small, bright circular objects – the fluorescent nuclei of apoptotic cells. This spot detection routine allows one to easily identify AO-positive cells and follow them over time. To generate a composite image showing the lifetime of each dying cell, 5-10 sequential spot detected images were then overlaid using a projection function (Deltavision, Applied Precision Issaqua, WA). This time projection method produces a tracing of the dying cell over time. The initial position of each dying cell was mapped onto the appropriate stage embryo (Hartenstein, 1993).

In situ hybridization

rpr cDNA was isolated and labeled as described previously (Namba et al., 1997). Embryos were processed as whole mounts as described by Tautz and Pfeifle (1989). Complexed probe was detected using an alkaline-phosphatase-conjugated antibody against the digoxigenin dUTP (Boehringer Mannheim). For double labeling experiments with *rpr* in situ probe and EN antibody, the in situ protocol was carried out first. The antibody staining was performed after dehydration with ethanol without xylene clearing.

Antibody staining

Embryos were processed as described by Bomze and Lopez (1994) using a anti-*en*/*inv* mouse monoclonal antibody diluted 1:1000 to visualize EN. Primary antibodies were visualized by using a goat anti-mouse secondary antibody and the ABC kit from Vector Labs.

TUNEL

Embryos were dechorionated and fixed for 20 minutes in 4% paraformaldehyde in PBS:heptane 1:1. Embryos were devitellinized by shaking in 80% ethanol and gradually rehydrated in PBS. Embryos were then washed once in reaction buffer consisting of 2.5 mM $CoCl_2$ and 1× terminal transferase (TdT) buffer (Boehringer Mannheim). For the terminal transferase reaction, embryos were incubated for 3 hours at 37°C in 2.5 mM $CoCl_2$, 1× TdT buffer, 5 μM dUTP, 5 μM CY3-dUTP (Amersham), 50 units TdT. Embryos were washed three times for 10 minutes in PBS plus 0.3% Triton X-100 and then processed with the ABC kit following standard protocols. After the reaction, embryos were washed four times for 15 minutes in PBS plus 0.3% Triton X-100 and probed with the EN antibody as described above. Embryos were viewed using a Texas Red filter to detect Cy3-labeled DNA fragments in the dying cells.

In these fluorescent images the *en* HRP-labeled cells appeared black on a gray background.

RESULTS

In vivo mapping of cell death in wild-type embryos

Embryonic cell death is a very dynamic process that starts during late stage 11 and continues through hatching of the embryo into a larva. Given the short lived nature of these apoptotic events, it is essential to use time-lapse microscopy to map cell death. Apoptosis can be monitored in living embryos by using the fluorescent vital dye acridine orange (AO) (Abrams et al., 1993). AO is stored in the lysosomes of living cells in a quenched state until the cell undergoes apoptosis. When a cell dies by apoptosis the AO is released from the lysosome and enters the nucleus where it binds to duplex DNA and becomes highly fluorescent (Delic et al., 1991). Time-lapse, fluorescence microscopy of apoptosis allows one to gain a complete picture of the spatial and temporal locations of all the cell deaths in a single embryo. To ensure that only epidermal cell death was scored, focal planes within 10 μm of the embryo surface were used for analysis. Fig. 1A shows a series of images from a wild-type embryo that has been injected with AO. Dying cells appear as small white spots in the black background. Scavenger cells or macrophages also become fluorescent after they engulf dying cells.

There were two problems associated with generating the cell death maps: the persistence of dead cells and interference from macrophages that engulf dying cells. The cell death map is intended to show the position of a cell when it first becomes AO positive. However, the AO-positive cells can persist in the epithelium up to 45 minutes before it is engulfed by neighboring cells or macrophages. This means that the same apoptotic cell will appear in up to 10 sequential images of a time-lapse recording. To prevent counting the same cell more than once, one must track each apoptotic cell over time. Tracking apoptotic cells is made more complicated by morphogenetic movement and engulfment by neighboring cells. To track AO-positive cells we used spot detection software and multiple time-point projections. The spot detection software identified all of the AO-positive cells in each image (Fig. 1B). Overlaying sequential spot-detected images revealed a tracing of AO-positive cells over time (Fig. 1C). The first point on this tracing provided the map location of when the each cell first became AO-positive and subsequent time-points in the track were used to avoid re-mapping the same cell. Tracking the apoptotic cells over time allowed us to follow these cells during germband retraction and dorsal closure, and their movement as they are engulfed by macrophage or neighboring cells.

The second problem with cell death mapping was that highly motile macrophages became fluorescent when they engulfed dying cells and thus complicated the images. Although macrophage are not as abundant in the ectoderm as

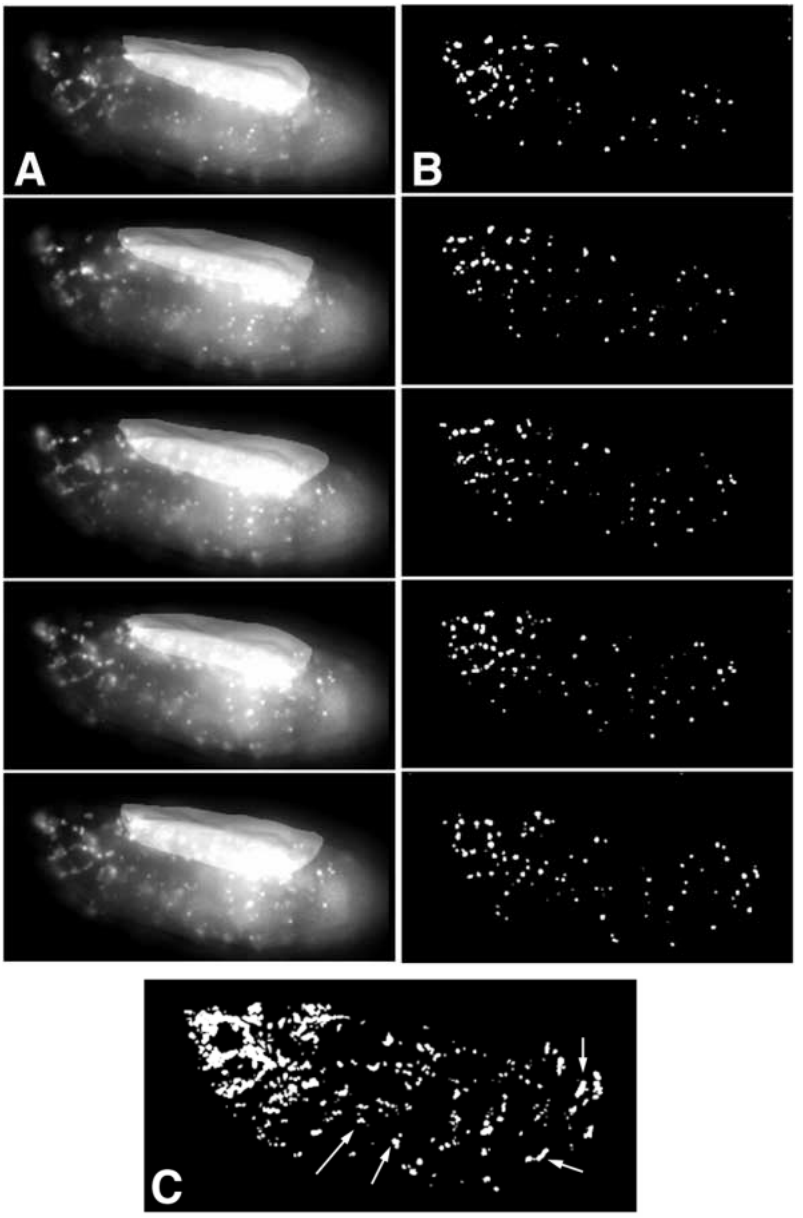

Fig. 1. Cell death mapping in wild-type embryos. (A) A series of 5 consecutive fluorescence, time-lapse images of an AO-injected wild-type embryo mounted laterally. Images were taken at 6 minute time intervals. Dying cells appear as small white spots in the dark background and macrophages appear as larger irregular shape spots. In this and all the remaining figures, except Fig. 4, anterior is to the left and dorsal is up. The autofluorescent yolk has been overlaid with a light-gray mask. (B) The same series of images as shown in A after being processed with the spot detection software. Each spot in these images represents either a dying cell or macrophage. (C) An overlay of the images from the five successive time points shown in B. Many of the dying cells move with the surrounding tissue, over time, forming a line of spots (posterior two arrows), while other dying cells move only slightly over time (anterior two arrows).

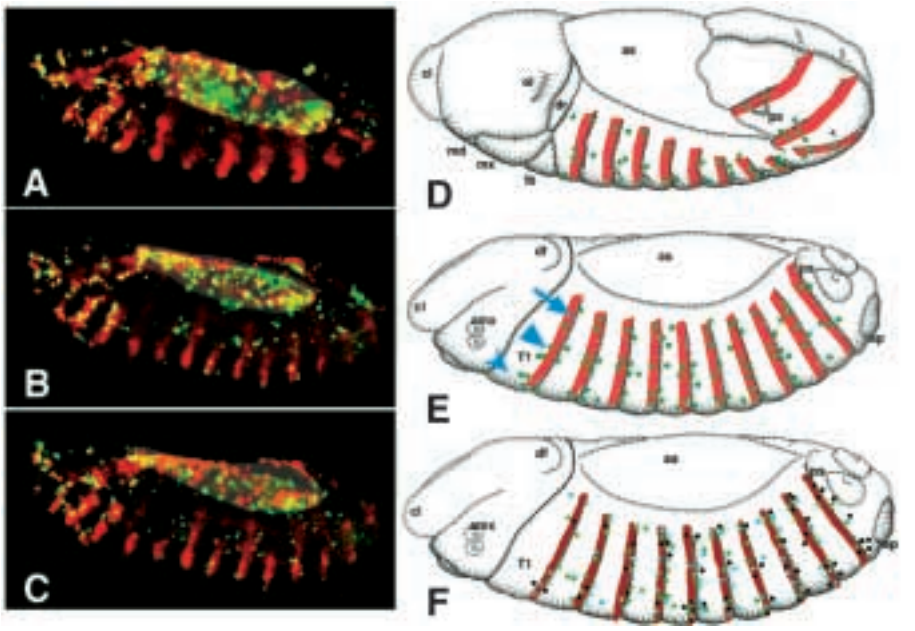

Fig. 2. Mapping cell death relative to *en:lacZ* expression. *en*:*lacZ* embryos were coinjected with AO and RGPEG. (A-C) Images from a time-lapse recording of an embryo at stage 12, 13 and 14; red shows *en* expression and green shows AO-positive cells. Using these landmarks and the spot detection procedure, maps of cell death spanning stages 12 to 14 were created. (D) A map of dying cells relative to *en* expression (the red stripes) prior to and during stage 12, superimposed on a sketch of a stage 12 embryo (Hartenstein, 1993). (E) A map of dying cells relative to *en* expression (the red stripes) during stages 13 and 14, superimposed on a sketch of a stage 14 embryo (Hartenstein, 1993). Arrow, dorsal cluster; arrowhead, mid-lateral cluster; concave arrowhead, ventrolateral cluster) (F) Comparison of cell death in three wild-type embryos at stage 13. Shown here are the results from three separate cell death mapping experiments using different embryos from that in A-E. Each colour represents a different embryo.

in the head and central nervous system, some are present. The macrophages can be distinguished from the dying cells because they are highly motile and larger than the dying cells and form paths that are not continuous or switch direction in the time-projected images. Macrophages can also be distinguished by the fact that they often have numerous bright spots within them, representing several engulfed apoptotic nuclei. These characteristics of macrophage have been described previously in fixed embryos (Tepass et al., 1994). Creating tracks of AO-positive objects allowed us to create a spatiotemporal map of the patterns of cell death in the embryonic epidermis.

In order to generate relational cell death maps, a variety of markers were used to indicate specific regions of the embryo. *en:lacZ* expression, which can be detected in living embryos by RGPEG injection (Minden, 1996), was used to indicate the posterior margin of the abdominal segments. Time-lapse recordings were made of *en:lacZ* embryos coinjected with AO and RGPEG (Fig. 2). Approximately three-quarters of the dying cells appeared in or immediately adjacent to the *en* stripe. The rest of the apoptotic nuclei were located in the middle of the segment. There was also an apparent clustering of apoptotic nuclei at specific locations along the dorsal-ventral axis (Fig. 2E). Examination of multiple embryos showed that the pattern of cell death in each embryo was similar, however the number of dying cells in each embryo and each segment varied from embryo to embryo (Fig. 2F). This variation indicates a plasticity in development, where each developing embryo can eliminate different numbers of cells depending on its own developmental circumstances. Approximately 12-16 cells die in the lateral region of each epidermal segment during stages 12-14. After stage 14, cell death in the abdominal ectoderm diminished.

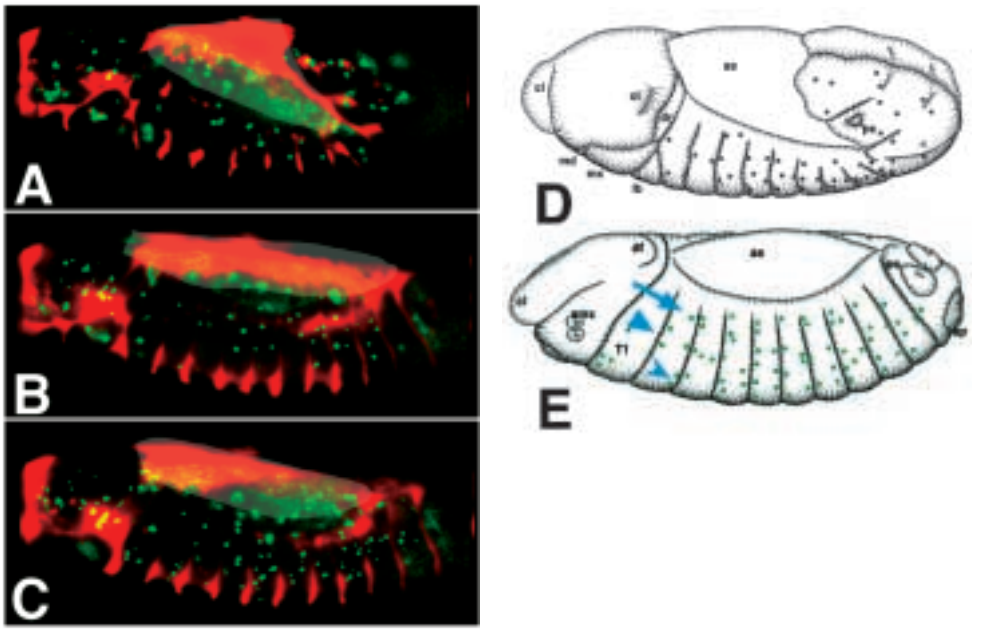

Fig. 3. Mapping cell death relative to segment borders. Embryos were injected with AO into the syncytial cytoplasm (green) and then injected with RGPEG into the intervitelline space to mark the segment borders (red). The large shaded area masks the signal due to yolk autofluorescence. (A-C) Images from a time-lapse recording of an embryo at stage 12, 13 and 14. (D) A map of abdominal epidermal cell deaths during stages 11-12. (E) A map of abdominal ectodermal cell death during stages 13-14. Arrows and arrowheads indicate the three clusters of death along the D-V axis.

Since β-galactosidase is a very stable protein, the early broad *en* expression domain remained at later stages and exaggerated the width of *en* expression. To corroborate the *en*:*lacZ* data, apoptosis was mapped with respect to the segment borders, which were visualized by injecting the embryos in the intervitelline space with RGPEG, which is cleaved by an uncharacterized β-galactosidase activity (Minden, 1996) (Fig. 3). Approximately three-quarters of the dying cells mapped adjacent to both sides of the segment border while the remainder were in the middle of the segment. In addition to the segmentally repeated cell death pattern, the majority of AO-positive cells appeared in roughly three clusters along the dorsal ventral axis (Fig. 3E).

Cells die in stripes in the ventral ectoderm

The limited axial resolution of the microscope prevents one from monitoring all dying cells throughout the embryo in a single recording. In order to map ectodermal apoptosis adjacent to the ventral midline, time-lapse recordings were made of ventrally oriented wild-type embryos. Intervitelline RGPEG recordings revealed that two rows of cells on either side of the segment border died in each segment of the ventral ectoderm during stages 12-14 (Fig. 4). There were approximately 6-8 dying cells in each row per hemi-segment. Similar to the lateral ectoderm, the precise location and number of dying cells was variable.

Accounting of cell death figures per segment

Quantitative analysis of the number of cell deaths per segment showed a definite bias toward apoptosis at the segment boundaries. We counted the number of cell deaths occurring within the 2-3 cells either side of the segment boundary and compared this with 5-6 cells in the middle of the segment. Considering that a segment is 10-12 cells across, this accounting partitions the segment into two equal-sized groups; the segment border cells and mid-segment cells. The segment border cells included the *en* cells plus one or two rows of cells anterior and two or three cell rows posterior to the *en* stripe. Analysis of four time-lapse recordings of wild-type embryos, where eight segments were scored per embryo, showed that 73% of cell death occurred in the segment border cells and the remaining 27% occurred in the mid-segment cells.

TUNEL labeling in the epidermis

The TUNEL method was used to label dying cells in fixed embryos to corroborate the *in vivo* results (White et al., 1994). The embryos were double labeled for *en* expression

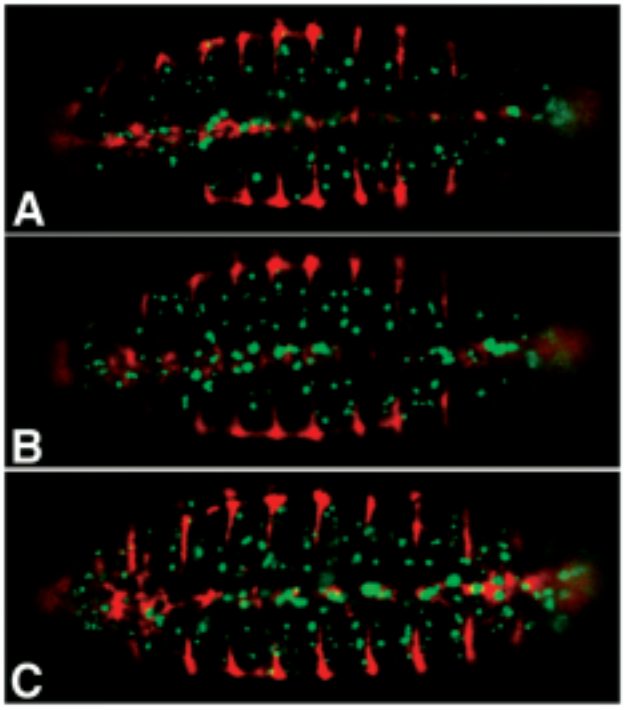

Fig. 4. Cell death in the ventral ectoderm. (A-C) Time-lapse images of a ventrally oriented embryo doubly injected with cytoplasmic AO and intervitelline RGPEG, at stage 12, 13 and 14. Macrophages appear as large cells predominantly along the ventral midline. Some of the macrophages appear to have taken up some of the intervitelline RGPEG as well as AO-positive cell bodies and appear as yellow cells containing both fluorophores. Anterior is to the left.

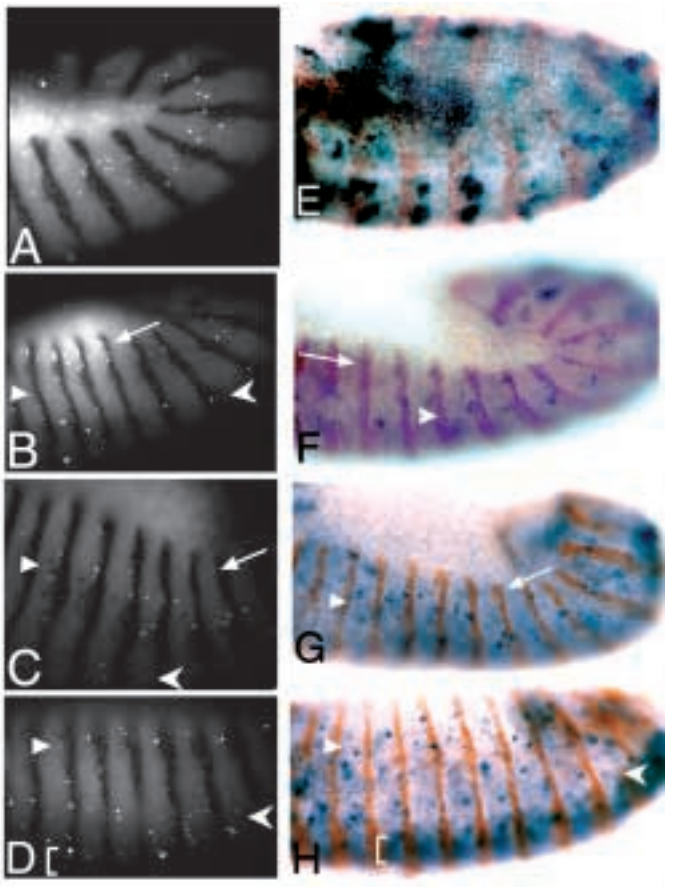

Fig. 5. Comparison of AO-positive cell death pattern to TUNEL and *rpr*-positive cell death patterns. (A-D) Images of mid stage 12, late stage 12, stage 13 and stage 14 embryos. The embryos have been double labeled for TUNEL (bright white spots) and *en* expression (black stripes). The bracket in D indicates the ventral cell death. (E-H) *rpr* expression (blue) and EN protein (brown) in wild-type embryos at stage 11, mid stage 12, stage 13 and stage 14, respectively. The bracket in H indicates out of focus *rpr* expression in the ventral ectoderm and CNS. The various types of arrow and arrowheads indicate the same D-V clusters of apoptotic cells as seen in the preceding Figs.

to highlight segment boundaries. TUNEL-positive nuclei were located throughout the segment and exhibited clustering along the dorsoventral axis similar to the in vivo results (Fig. 5A-D). The number of TUNEL-positive nuclei at a single time point was similar to that seen in individual AO images except in the ventral epidermis where there were fewer TUNEL-positive nuclei. The earliest cell deaths, at stage 12, occurred more frequently in the mid-segment cells (Fig. 5A). However, when scoring for cell death over time, we found about two-thirds of the dying cells were located in the segment border cells; one-third of the apoptotic nuclei were seen in the mid-segment, where 12 embryos between stages 12-14 were analyzed. Considering that TUNEL labeling is a static technique, we cannot determine if the location of the dying cells in these images is the precise position at which the cell first becomes apoptotic. In the time-lapse AO recordings, apoptotic cells that originated in the *en:lacZ* stripes were seen to move anteriorly relative to the *en* stripe, indicating the engulfment of the dead cells by their anterior neighbors. Epidermal cells have been shown previously to engulf dead neighbors (Tepass et al., 1994). The engulfment of the segment border cells by their mid-segment neighbors could explain the relative increase in mid-segment TUNEL-positive cells since TUNEL also labels engulfed nuclei. These results demonstrate that programmed cell death occurs in a stereotypical pattern in the lateral ectoderm.

Cells adjacent to the epidermal segment border express *rpr*

Previous experiments have indicated that expression of *rpr* correlates with the pattern of dying cells in the embryo and precedes AO signal by 2 hours (White et al., 1994). In situ hybridization to *rpr* mRNA was performed in an attempt to correlate *rpr* expression with the in vivo cell death maps. *rpr* expression at early stage 11 was in large patches in the ventral epidermis (Fig. 5E). The number of cells expressing *rpr* at stage 11 was greater than the number of AO-positive cells that were seen throughout epidermal development. Lack of correlation between the number of *rpr*-expressing cells and AO-positive cells at this stage can be explained in two ways. (1) Some cells in the epidermis that express *rpr* at stage 11 do not become AO-positive, but still apoptose. (2) Some of the stage 11 *rpr*-expressing cells do not enter apoptosis and become AO-positive. We prefer the latter explanation, given that the AO and TUNEL results correlate. At late stage 12 and stages 13-14 the expression of *rpr* in the epidermis correlated fairly well with the cell death pattern observed with AO (Fig. 5 F-H). Quantifying these results showed a good spatial correlation between later *rpr* expression and AO-positive cells both in the lateral ectoderm. In the lateral ectoderm during late stage 12 to stage 14, approximately two-thirds of the *rpr*-positive cells were in the segment border region; 30 embryos were scored. Although relative numbers of *rpr*-positive and AO-positive cells were similar at similar time points, an exact quantitative comparison cannot be performed due to the static nature of the *rpr* analysis. Previous results have suggested that *rpr* expression precedes cell death by 2 hours (White et al., 1994), however our results show a better correlation with AO data at similar developmental stages.

Cell death in segment polarity mutants of the *wg* class

Since the pattern of cell death correlated with segment polarity gene expression, we examined the role that these genes play in establishing the abdominal epidermal cell death pattern. Strong mutations in segment polarity genes lead to the production of larvae that are smaller than wild-type (Perrimon and Mahowald, 1987; Klingensmith et al., 1989). It has been proposed that this reduction in larval size is a result of increased cell death in the embryo. If there is extra cell death in segment polarity mutants, then the segment polarity genes must play a role in maintaining epidermal cell viability. To investigate this further we examined apoptosis in segment polarity mutants.

The development of the epidermis can be divided into two phases. Signaling between WG and EN cells is required during stages 9 and 10 to stabilize segment polarity gene expression throughout the segment. During stages 11 and 12, WG signaling is required to establish cell fates throughout the segment (Bejsovec and Martinez Arias, 1991; DiNardo et al., 1994). Time-lapse analysis of strong alleles of *wg*, *en* and *arm* showed extensive cell death throughout the abdominal epidermis as well as other embryonic tissues (data not shown). Since these mutations altered epidermal development early in the stabilization phase, we analyzed cell death in temperature sensitive mutants to monitor the effects of loss of WG and ARM function during either the stabilization phase or the fate specification phase.

$wg^{1\text{-}12}$ (referred to as wg^{ts}) produces functional WG at the permissive temperature of 17°C. At the non-permissive temperature, >20°C, WG protein fails to be secreted (Gonzalez et al., 1991). wg^{ts} embryos were collected at the permissive temperature and syncytial embryos were injected with AO. The embryos were then incubated at the permissive temperature until stage 9, approximately 4.5 hours after injection. The embryos were then shifted to the non-permissive temperature of 25°C, and time-lapse recordings were made 2 hours later at 22°C. A series of time-lapse images from such a movie is shown in Fig. 6A-C. Massive cell death was seen throughout the embryo. The most obvious increase in cell death was seen at the tip of the germband and in the epidermis. It is important to note that although there was a dramatic increase in cell death throughout the epidermis, many regions of the epidermis exhibited little or no cell death. Under these conditions, WG secretion was inhibited during the stabilization phase of epidermal patterning, which affects overall patterning of the epidermis. The widespread cell death was likely to be an indirect effect of general pattern disruption and not a direct result of the WG signal promoting cell survival.

In order to determine if WG plays a role in providing a trophic signal to specific cells, wg^{ts} embryos were shifted to the non-permissive temperature at stage 11, during the fate specification phase of epidermal development. In order to examine cell death during this stage of epidermal development, wg^{ts} embryos were injected with AO and incubated at the permissive temperature until stage 11, 6.5 hours after injections and then time-lapse recordings were immediately started at the non-permissive temperature. Under these conditions, there was a significant increase in cell death that appeared as stripes about 2-3 cells in diameter in each segment during stages 12-14 (Fig. 6D-F).

Intervitelline RGPEG injections showed that the dying cells were located in the anterior half of the segment near the segment border (Fig. 6G). Given the abundance and concentration of cell deaths in these mutants, we were unable to perform an exact time-lapse quantitative analysis using the tracking method. However, a comparison of the wild-type and mutant embryos at the same stage showed a 5-fold increase in the number of dying cells in the anterior of the segment. The level of cell death in the remainder of the segment appeared to be unaffected. The embryos were allowed to develop to late stage 17 and their cuticle patterns were analyzed to confirm that embryos with the increased cell death pattern were *wg* mutants. Embryos with increased cell death at the segment border consistently exhibited a *wg* cuticle phenotype.

Cell death in an *armadillo* temperature sensitive mutant

ARM, a β-catenin homolog, functions both in the adhesion junctions and in WG signal transduction (Peifer and Wieschaus, 1990). In order to examine the role of ARM in cell survival, we examined cell death in *arm* mutant embryos. A temperature sensitive mutation was used to precisely control the time at which ARM signaling was removed. The temperature sensitive mutant, $arm^{H8.6}$ (referred to as arm^{ts}) is primarily defective in WG signal transduction (Klingensmith et al., 1989). arm^{ts} embryos were collected at room temperature (22°C), injected with AO and immediately shifted to the restrictive temperature of 29°C and aged until stage 11, at which point time-lapse recordings were initiated at room temperature. Cell death increased in the same rows of cells as seen in wg^{ts} embryos that were shifted to the restrictive temperature at stage 11 (Fig. 7A-B). Cell death in the rest of the segment was similar to wild-type. The width of the stripe of cell death expanded posteriorly, toward the middle of the segment, in embryos that were collected at 25°C, instead of 22°C (data not shown). These embryos also had a slight increase in cell death in the posterior of the segment in the *en*-expressing cells. The homozygous arm^{ts} embryos that were collected at 25°C had more severe cuticle defects than those collected at 22°C, which correlated with the width of the cell death stripe. These results are consistent with the *wg* result and indicate that the transduction of the WG signal through the ARM pathway is required to promote cell survival of rows of cells in the anterior half of the segment.

Cell death in *gsb* mutant embryos

Previous studies have shown that *gsb*, which encodes for a transcription factor, functions in an autoregulatory loop required for the maintenance of WG expression (Li and Noll, 1993). More recently, it has been proposed that GSB is specific to the ventral epidermis for the maintenance of WG expression and that another transcription factor, *ladybird*, provides the corresponding function in the dorsal epidermis (Jagla et al., 1997). It was reasoned that loss of *gsb* may only lead to the demise of cells in the ventral epidermis. This was examined by time-lapse microscopy of AO and intervitelline RGPEG-injected embryos that had both *gsbd* and *gsbp* genes deleted. Mutant embryos were identified by cuticle analysis of the mounted embryos. *gsb* mutant embryos displayed an increase in apoptotic nuclei in the anterior portion of the segment similar to that seen in wg^{ts} and arm^{ts} embryos (Fig. 7C-D). However, the increase in cell death was restricted to the ventral and ventrolateral surface of the embryo. There was also a slight increase in cell death in the ventral EN-expressing cells.

Cell death in *nkd* mutant embryos

Mutations in the segment polarity gene, *nkd*, also resulted in increased cell death that appeared in a striped pattern in the abdominal epidermis (Fig. 7E). Intervitelline RGPEG indicated that the cells that were dying were in the extreme posterior of the segment where *en* is expressed. The segment borders were shallow and in some cases ran together between adjacent segments. We used TUNEL to localize the cell death in *nkd* mutants relative to *en* expression to show that the majority of the increased cell death was in the *en*-expressing cells (Fig. 7F-G). The *nkd* embryos had about a 6-fold increase in apoptosis in EN cells compared to similar staged wild-type embryos. The domain of EN expression was expanded anteriorly in *nkd* mutants, which was where the increased cell death was located. There was also a slight increase in cell death throughout the segment.

DISCUSSION

Cell death in wild-type embryos is segmentally repeated

Programmed cell death in *Drosophila* embryos starts at late stage 11 and continues throughout embryonic development. Using time-lapse microscopy of AO-injected embryos, we have analyzed the cell death patterns in the abdominal epidermis to show that approximately 40-45 cells die in the ectoderm of each segment during stages 12-14. The number of dying cells varies from embryo to embryo although the relative location of the dying cells is consistent. The fact that cells die in similar positions in different embryos indicates that precise mechanisms are employed to select the doomed cells. The variation in cell death numbers may reflect fluctuations in the number of cells in the abdomen of different embryos and variability in pattern formation. It is believed that the role of cell death is to remove excess cells at the end of a patterning process, such as is the case in *Drosophila* eye development (Cagan and Ready, 1989). We have previously shown that increasing or decreasing the number of cells fated to the abdomen was repaired by increased or decreased abdominal cell death, respectively, which resulted in normalized abdominal patterning (Namba et al., 1997).

Double labeling for cell death and segment boundaries was used to spatially locate dying cells within each segment. The majority of the apoptotic nuclei lay within a few cell diameters of either side of the segment border. This corresponds to the region in or adjacent to *en* expression. Mapping cell death with respect to *en* expression provided similar results where approximately three quarters of the dying cells mapped in or adjacent to *en* expression. This bias in the location of cell death was independent of whether dying cells were identified by TUNEL, *rpr* expression or AO. The segmental pattern of cell death implicated the segment polarity genes in establishing the wild-type cell death pattern. The segment polarity gene

products are known to be essential in establishing cell-cell communication that is responsible for generating epidermal fates (reviewed by DiNardo et al., 1994). Perhaps this cell-cell communication is also required for cell survival as well as determining cell fate.

Segment polarity mutants of the WG class have increased cell death in the anterior of the segment

Increased cell death has often been implicated in mutations that affect segment polarity genes resulting in smaller larvae (Perrimon and Mahowald, 1987; Klingensmith et al., 1989). Time-lapse microscopy of AO-injected embryos mutant for genes in the WG signaling pathway was performed to determine precisely when and where cells die in these mutants. In order to gain better control over the stage at which the WG expression was lost, we used a temperature sensitive mutation of *wg*. Cell death in wg^{ts} mutant embryos shifted to the restrictive temperature at stage 9 was increased dramatically in many regions of the embryo, making it difficult to ascertain any specific cell death pattern. This abundant cell death is likely to be a result of an overall defect in pattern establishment. In spite of the early stage 9 loss of *wg* expression, the increase in cell death was not observed until stage 12, during germband retraction. The restriction of cell death to after stage 11 or 12 in these mutants and in wild-type embryos indicates developmental regulation of cell death competence. Despite the extensive cell death in wg^{ts} embryos that were shifted to the restrictive temperature at stage 9, many cells did not undergo apoptosis, indicating that the survivors were either unaffected by the loss of WG signaling or they were resistant to apoptosis.

When WG function was disrupted during stage 11, the fate specification phase of epidermal development, approximately two rows of cells died in the anterior-most portion of each segment during stages 12-14 (Fig. 6). These dying cells were approximately 6 rows of cells away from the WG-secreting cells. An *arm* mutation that disrupted WG signaling also eliminated the same rows of cells. These results show that WG signaling is required at a distance to promote the survival of cells in the anterior of the segment. It is important to note that the cells expressing WG prior to the temperature shift and those cells immediately anterior to WG-secreting cells did not die and, therefore, may be more resistant to apoptosis than those cells at a distance. Mutations in the segment polarity genes *gsb* also led to the death of cells in the anterior of the segment. However this death was more restricted to the ventral surface.

Apoptosis in *nkd* mutants

Strong mutations in *nkd* results in a cuticle phenotype opposite to that of *wg* mutations. Previous genetic studies have suggested that the *nkd* gene product is necessary to suppress the domain of WG function. *nkd* mutants also have increased cell death, of which the majority is in the expanded EN-expressing domain. There is however no increase in cell death in the anterior of the segment similar to that seen in WG mutants. Taken together these results suggest that two separate systems may be involved in promoting cell survival in the embryonic ectoderm: a *nkd*-dependent system that keeps posterior cells alive and a *wg*-dependent system that plays a similar role in the anterior of the segment. These two systems may not be mutually exclusive. It has been suggested that cell death in a *wg* mutant is suppressed by a *nkd* mutation (Bejsovec and Wieschaus, 1993). These results provide evidence that segment polarity gene interactions play an intimate role in epidermal cell survival. However, much more work is needed to further our understanding of these processes.

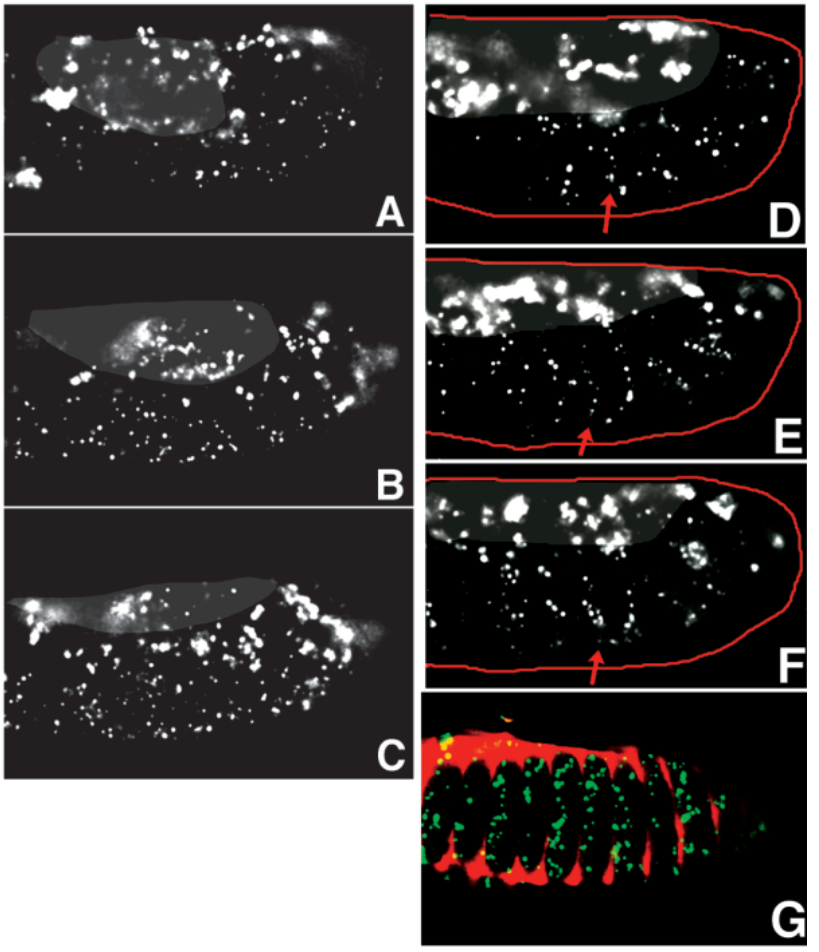

Fig. 6. Cell death in wg^{ts} embryos shifted to the restrictive temperature at stage 9, during the stabilization phase. Embryos from wg^{ts}/Cy (*ftz*:*lacZ*) were injected with AO, aged at the permissive temperature for 4.5 hours and then shifted to the restrictive temperature. (A-C) Time-lapse images of the same embryo at stage 12, 13 and 14. Cell death in wg^{ts} embryos shifted to the restricted temperature at stage 11. wg^{ts} embryos were injected with AO and aged at the permissive temperature for 6.5 hours until stage 11 and then shifted to the restrictive temperature. (D-F) Selected images from a time-lapse recording of a wg^{ts} embryo at stage 12, 13 and 14. Only the abdomen is shown. The red arrows indicate continuous stripes of cell death. (G) Double injection of wg^{ts} embryos with intervitelline RGPEG (red) and cytoplasmic AO (green) shows that the increased cell death is near the anterior segment border in approximately two rows of cells along the dorsal-ventral axis.

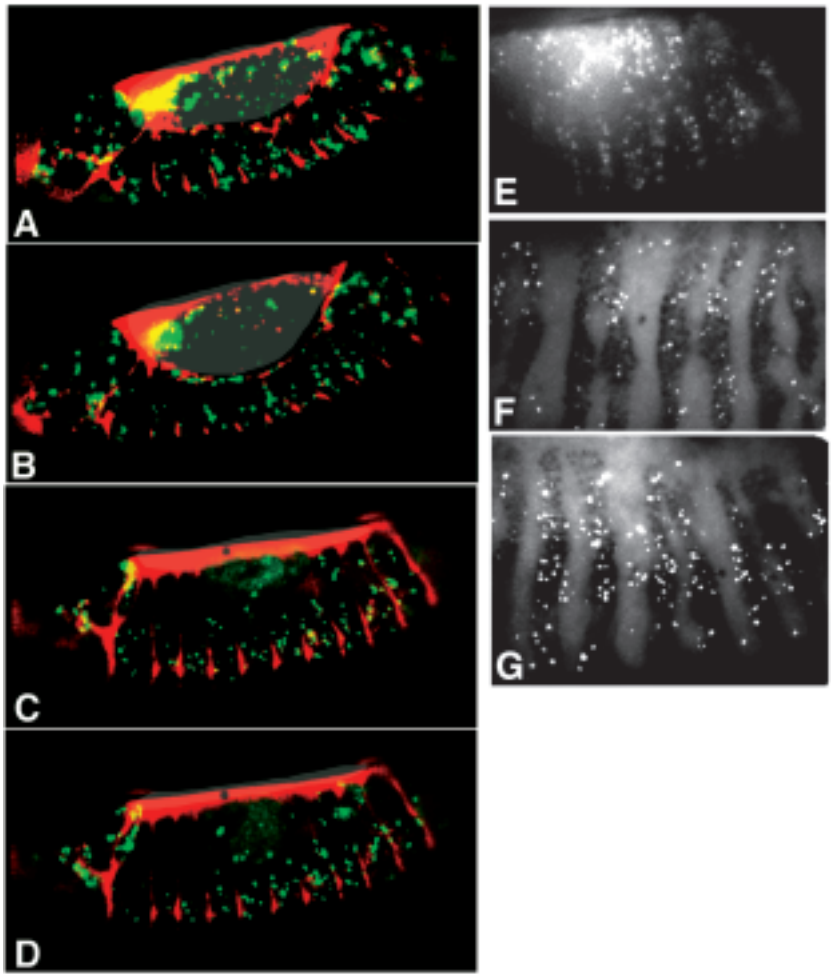

Fig. 7. Cell death patterns in *arm*, *gsb* and *nkd* mutant embryos. (A-B) Images from a time-lapse recording of an arm^{ts} embryo at stage 12 and 13 shifted from 22°C to the restricted temperature at stage 5. AO-positive signal, or dying cells are shown in green and the segment borders are in red. This embryo is slightly rotated to show more of the dorsal surface. (C-D) Images from a time-lapse recording of a *gsb* embryo at stage 12 and 13. Notice the increased cell death at the anterior segment border. The majority of the ectopic cell death was restricted to the ventral half of the embryo. (E) An image of the abdomen of a stage 13 *nkd* mutant embryo injected with AO. (F-G) A *nkd* mutant embryo at late stage 12 and 13 that has been double labeled with TUNEL and anti-EN antibody.

How does the removal of WG cause cell death in the anterior of the segment?

As stated above, there is a significant separation between the WG-secreting cells and the cells that die in response to loss of WG signaling. One possible explanation is that WG acts directly on these cells by diffusing over a large distance to promote cell survival. When WG is removed, the cells die. The cells adjacent to the WG cells may still receive sufficient signal to survive. There is some debate as to how far the WG signal can be transmitted across the segment. Previous results suggest that the WG signal is only able to directly affect the fate of cells adjacent to the WG secreting cells, only one or two rows away (Vincent and Lawrence, 1994). Lawrence et. al (1996) proposed a model where a steep gradient of secreted WG plays a role in promoting cell survival. Another possible explanation for the long-range WG effect is that WG is acting through an intermediate signal that is produced by cells receiving a short-range WG signal – this is a relay mechanism. When WG-responding cells adjacent and anterior to WG-secreting cells are disturbed, there is a disruption of a signal that promotes the survival of even more anterior cells. The fact that mutations in *arm* lead to the same cell death phenotype as wg^{ts} mutants and that there is no indication of nuclear ARM accumulation in the anterior-most cell of the segment, suggests that the survival of the anterior-most cells may be dependent on a different factor that is secreted in an ARM-dependent fashion.

The time and location of epidermal cell death in the wild-type embryo indicates that cells are selected to die during the stage that WG and EN cells are signaling to each other to establish epidermal cell fates. Our results indicate that one of the roles of this signaling is to establish cell survival. Cells that do not receive the appropriate signal or signals at the appropriate time die by apoptosis. Furthermore, our results suggest that complex cell-cell interactions are essential to promote cell survival within segments of the abdominal epidermis. Cell-cell interactions also seem to play a role in promoting cell survival in the wing disc. Cell ablation in one region of the wing disc leads to apoptosis of cells in adjacent territories (Milán et al., 1997). The results presented here only examine the effects of removing signals from a few rows of epidermal cells. Interactions between other rows of epidermal cells will certainly be important for promoting cell survival. Future experiments will need to be performed to further address the role of cell-cell communication in the survival of abdominal ectoderm cells. These results also provide a basis in furthering our knowledge on how epidermal mutant phenotypes evolve and how the segment polarity genes function in normal embryos. *wg* mutants are devoid of smooth cuticle and have several rows of type four denticles. Our results

suggest that one requirement for this phenotype is the death of anterior row cells, which produce type two and three denticles. Future experiments will examine the role of cell death in generating these mutant phenotypes.

We would like to thank Steve DiNardo for the wg^{ts} flies and the EN/INV antibody and Norbert Perrimon for the arm^{ts} fly stock. We would also like to thank Brian McNally and Wladimir Labeikovsky for their technical help and Minako Pazdera for her support. T. P. was supported in part by an NSF graduate training Grant to the Science and Technology Center for Light Microscope Imaging and Biotechnology, BIR 9256343. J. M. is a Lucille P. Markey Scholar, and this work was supported in part by grants from the Lucille P. Markey Charitable Trust and NIH grant HD31642.

REFERENCES

Abrams, J. M., White, K., Fessler, L. I. and Steller, H. (1993). Programmed cell death during *Drosophila* embryogenesis. *Development* **117**, 29-43.

Bejsovec, A. and Martinez Arias, A. (1991). Role of *wingless* in patterning the larval epidermis of *Drosophila*. *Development* **113,** 471-485.

Bejsovec, A. and Wieschaus, E. (1993). Segment polarity gene interactions modulate epidermal patterning in *Drosophila* embryos. *Development* **119**, 501-517.

Bomze, H. M. and López, A. J. (1994). Evolutionary conservation of the structure and expression of alternatively spliced *ultrabithorax* isoforms from *Drosophila*. *Genetics* **136**, 965-977.

Cagan, R. L. and Ready, D. F. (1989). The emergence of order in the *Drosophila* pupal retina. *Dev. Biol.* **136**, 346-362.

Campos-Ortega, J. A. and Hartenstein, V. (1985). The embryonic development of *Drosophila melanogaster*. New York, Berlin, Heidelberg, Tokyo: Springer-Verlag.

Delic, J., Coppey, J., Magdelenat, H. and Coppey-Moisan, M. (1991). Impossibility of acridine orange intercalation in nuclear DNA of the living cell. *Exp. Cell. Res.* **194**, 147-153.

DiNardo, S., Heemskerk, J., Dougan, S. and O'Farrell, P. H. (1994) The making of a maggot: patterning the *Drosophila* embryonic epidermis. *Cur. Opin. Gen. Dev.* **4**, 529-534.

Edgar, B. A. and Lehner, C. F. (1996). Developmental control of cell cycle regulators: a fly's perspective. *Science*. **274:**5293, 1646-1652.

Foe, V. E. (1989). Mitotic domains reveal early commitment of cells in *Drosophila* embryos. *Development.* **107**, 1-22.

Gonzalez, F., Swales, L., Bejsovec, A., Skaer, H. and Martinez Arias, A. (1991). Secretion and movement of *wingless* protein in the epidermis of the *Drosophila* embryo. *Mech. Dev.* **35**, 43-54.

Grether, M. E., Abrams, J. M., Agapite, J., White, K. and Steller, H. (1995). The *head involution defective* gene of *Drosophila melanogaster* functions in programmed cell death. *Genes Dev.* **9**, 1694-1708.

Hartenstein, V. and Campos-Ortega, J. A. (1985). Fate-mapping in wild-type *Drosophila Melanogaster* I. The pattern of embryonic cell divisions. *Wilhelm Roux's Arch. Dev. Biol.* **194**, 181-195.

Hartenstein, V. (1993). In *Atlas of* Drosophila *Development*. Cold Spring Harbor, NY: Cold Spring Harbor Laboratory Press.

Jacobson, M. D., Weil, M., and Raff, M. C. (1997). Programmed cell death in animal development. *Cell* **88**, 347-354.

Jagla, K., Jagla, T., Heitzler, P., Dretzen, G., Francois, B., and Bellard, M. (1997) *ladybird*, a tandem of homeobox genes that maintain late *wingless* expression in terminal and dorsal epidermis of the *Drosophila* embryo. *Development.* **124**, 91-100.

Klingensmith, J., Noll, E., and Perrimon, N. (1989). The segment polarity phenotype of *Drosophila* involves differential tendencies toward transformation and cell death. *Dev. Biol.* **134,** 130-145.

Lawrence, P. A., Sanson, B., and Vincent, J. P. (1996). Compartments, *wingless* and *engrailed*: patterning the ventral epidermis of *Drosophila* embryos. *Development*. **122,** 4095-4103.

Li, X. and Noll, M. (1993). Role of the *gooseberry* gene in *Drosophila* embryos: maintenance of *wingless* expression by a *wingless-gooseberry* autoregulatory loop. *EMBO J.* **12**, 4499-4509.

Martinez-Arias, A. (1993). Development and patterning of the larval epidermis of *Drosophila*. In *The Development of* Drosophila melanogaster (ed. Bate, M. and Martinez-Arias, A.), pp. 517-608. Cold Spring Harbor, NY: Cold Spring Harbor Laboratory Press.

Milán, M., Campuzano, S., and García-Bellido, A. (1997). Developmental parameters of cell death in the wing disc of *Drosophila. Proc. Natl. Acad. Sci. USA.* **94**, 5691-5696.

Minden, J. S. (1996). Synthesis of a new substrate for detection of *lacZ* gene expression in live *Drosophila* embryos. *BioTechniques* **20**, 122-129.

Namba, R., Pazdera, T. M., Cerrone, R. L., and Minden, J. S. (1997) *Drosophila* embryonic pattern repair: how embryos respond to *bicoid* dosage alteration. *Development* **124**, 1393-1403.

Nüsslein-Volhard, C. and E. Weischaus. (1984). Mutations affecting the pattern of the larval cuticle in *Drosophila Melanogaster*. I. Zygotic loci on the second chromosome. *Wilhelms Roux's Arch. Dev. Biol.* **193**, 267-282.

Peifer, M. and Wieschaus, E. (1990). The segment polarity gene *armadillo* encodes a functionally modular protein that is the *Drosophila* homolog of human plakoglobin. *Cell* **63**, 1167-1178.

Perrimon, N. and Mahowald, A. (1987). Multiple functions of segment polarity genes in *Drosophila. Dev. Biol.* **119,** 587-600.

Perrimon, N. (1989) Multiple functions of a *Drosophila* homeotic gene zeste-white 3, during segmentation and neurogenesis. *Dev. Biol.* **135**, 287-305.

Tautz, D. and Pfeifle, C. (1989). A non-radioactive in situ hybridization method for the localization of specific RNA's in *Drosophila* embryos reveals translational control of the segmentation gene *hunchback*. *Chromosoma* **98**, 81-85.

Tepass, U., Fessler, F. I., Aziz, A., and Hartenstein, V. (1994). Embryonic origin of hemocytes and their relationship to cell death in *Drosophila*. *Development*. **120**, 1829-1837.

Vincent, J. P. and Lawrence, P. A. (1994). Drosophila *wingless* sustains *engrailed* expression only in adjoining cells: evidence from mosaic embryos. *Cell.* **77**, 909-915.

White, K., Grether, M. E., Abrams, J. A., Young, L., Farrell, K. and Steller, H. (1994). Genetic control of programmed cell death in *Drosophila. Science* **264**, 677-683.